Dependency of IAM Losses in Colored BIPV Products on the Refractive Index of Colorants

Babin, Markus; Thorsteinsson, Sune; Santamaria Lancia, Adrian Alejo; Poulsen, Peter Behrensdorff; Thorseth, Anders; Dam-Hansen, Carsten; Jakobsen, Michael Linde

Published in:
Proceedings of 38th European Photovoltaic Solar Energy Conference and Exhibition

Link to article, DOI:
10.4229/EUPVSEC20212021-4BO.4.2

Publication date:
2022

Document Version
Publisher's PDF, also known as Version of record

DEPENDENCY OF IAM LOSSES IN COLORED BIPV PRODUCTS ON THE REFRACTIVE INDEX OF COLORANTS

Markus Babin*, Sune Thorsteinsson, Adrian A. Santamaria Lancia, Peter B. Poulsen,
Anders Thorseth, Carsten Dam-Hansen, Michael L. Jakobsen
Department of Photonics Engineering, Technical University of Denmark
Frederiksborgvej 399, 4000 Roskilde, Denmark
*Corresponding Author: marbab@fotonik.dtu.dk

ABSTRACT: Measurements of the incidence angle modifier (IAM) of colored PV modules based on inkjet-printed glass have shown differences between colors, which are uncorrelated with the total transmittance and reflectance of the colored glass. In this paper, the complex refractive index of ceramic inks is estimated based on measurements of reflectance and transmittance spectra. These estimates are used in ray-tracing simulations to determine the IAM of coupon-sized PV modules with printed ceramic inks. Comparisons of the simulation results to measured IAMs show a high correlation between the refractive index of colorants and the IAM.
Furthermore, estimations of the impact of IAM on performance based on TMY data at different locations are performed. The results indicate that changes in IAM due to sample coloration can lead to annual irradiance losses of up to 5% compared to uncolored glass. These losses are caused by additional reflections at the glass-ink interface according to the Fresnel equations, dependent on the refractive index of the ceramic inks.
Keywords: Building Integrated PV (BIPV), Optical Losses, Performance, Ray Tracing, Color

1 INTRODUCTION

Building-integrated photovoltaics (BIPV) present a huge potential market for PV deployment and its costs are already approaching competitiveness with conventional building materials. [1] Furthermore, BIPV eliminates the need for increased land usage and, due to its distributed nature, reduces the need for grid expansion by achieving physical proximity between generators and loads. [2]

One major barrier limiting the deployment of BIPV are aesthetic requirements, e.g. through building codes in city centers or cultural heritage sites. This issue is tackled by a variety of coloration technologies attempting to tailor BIPV appearance to the architectural requirements.

Coloration is usually achieved through spectrally selective absorption and reflection in a material between the glass cover and the PV cell, or through thin-film coatings leading to constructive or destructive interference of reflected light. Absorptive materials, either printed on the glass cover or introduced within the laminate have shown to achieve better color saturation and color constancy independent of incidence or view angle, but a significantly higher transmission loss compared to thin film coatings. [3] Nevertheless, most colored BIPV solutions on the market currently rely on this technology.

In a previous comparison of differently colored, inkjet-printed glasses, a significant difference in angular dependent transmittance – described by the incidence angle modifier (IAM) – was observed. This phenomenon is however correlated with neither the total transmittance at normal incidence, nor the primary wavelength of reflected or transmitted light. [3] As a possible alternative factor, this paper therefore investigates the correlation between the spectrally varying refractive index of the ceramic ink colorant and the measured IAM.

2 METHODOLOGY

For this paper, reflectance and transmittance spectra are measured on printed glass samples and used to estimate the wavelength dependent complex refractive index of the colorants. This data is then used as input in raytracing simulations used to predict the IAM of PV laminates with said colored glass. The simulation results are subsequently compared to measurements of the IAM of laminated samples. Finally, calculations based on TMY data are carried out to estimate the impact of the measured IAM on annual PV yields.

2.1 Sample preparation

In total, seven coupon-sized samples are investigated. The sample cover consists of a 200x300x3.5 mm low-iron float glass with ceramic ink printed on the inner side. The colored layer has a thickness of approximately 20 µm and is printed using a DipTech inkjet printer and thermally fused with the glass. The layer is printed in five primary colors (white, blue, green, red, yellow) and one compound color (terracotta).

The printed glasses (printed side facing the laminate) are used as superstrate for single-cell modules featuring mono-Si cells laminated on a black polymeric backsheet with EVA as encapsulant.

2.2 Measurements of the IAM

The main illuminating light source for all measurement setups is an Energetiq EQ-99X laser-driven light source (LDLS). This light source emits broadband light with high temporal stability. The light is collimated using three off-axis parabolic mirrors and an aperture to filter for divergent light. Furthermore, the setup includes a long-pass UV filter with a cut-off wavelength at 320 nm.

The samples themselves are mounted in a rotary stage with stepper motor, with a rotational axis aligned with the center of the light beam, allowing accurate variations of the incidence angle. I_{sc} of samples is determined through measurements of the voltage across a 0.5 Ω shunt resistor, with measurements averaged over 20 individual acquisitions to reduce noise. Simultaneously the temperature is monitored through a J-type thermocouple affixed to the center of the module backside. A schematic of the measurement setup is shown in Figure 1.

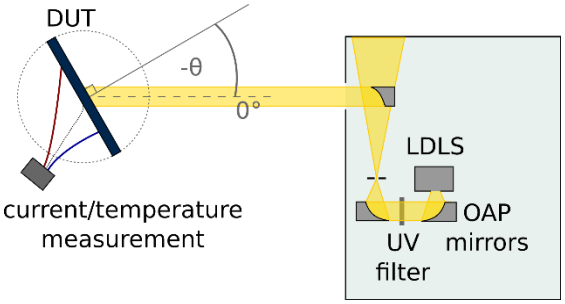

Figure 1: Setup for IAM measurements

For measurements of the IAM, an aperture of 10 mm diameter is placed within the collimated beam, so that the spot of incident light can be contained within the PV cell at all measured angles. This alleviates the need for cosine corrections, as the total incident flux on the sample is kept constant for all angles. Even though the cell is not fully illuminated as prescribed in the IEC 61852-2 standard [4], the measurement method shows high accuracy, as has been validated through inter-laboratory comparison. [5]

Four measurements in 5° steps are carried out per sample and averaged, including averaging over positive and negative incidence angles. In addition to the absolute IAM, a relative IAM is determined for colored samples as a relative measure compared to the unprinted reference:

$$rel.\ IAM_{sample} = \frac{IAM_{sample}}{IAM_{reference}}$$

2.3 Measurements of reflectance

For reflectance measurements, a 2” integrating sphere is used to capture both specular and diffuse reflections from the sample. For this, the collimated light from the LDLS is reflected towards the input port located at 4° compared to the surface normal. The reflected light is collected in the sphere and transferred to an OceanOptics QE65000 spectrometer using a 600 µm optical fiber, as can be seen in Figure 2. This spectrometer allows measurements of the spectral flux between approximately 200 and 980 nm with varying integration times.

The incident light is characterized using a LabSphere Spectralon reflectance standard with known spectral reflectivity. Subsequently, reflectance is measured on samples with the inkjet printed side facing towards the integrating sphere. A black backsheet is placed several mm below the glass surface to avoid additional reflections from transmitted light.

For each measurement, five spectra are acquired with five seconds integration time each and averaged, to reduce measurement noise. Additionally, for each measurement, dark signal spectra are acquired and subtracted.

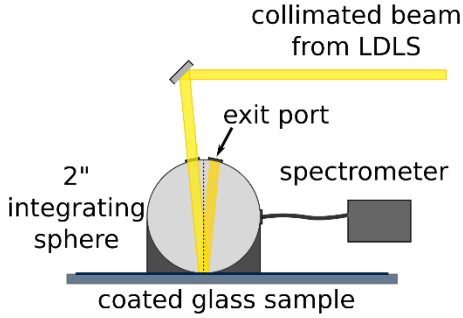

Figure 2: Setup for reflectance measurements

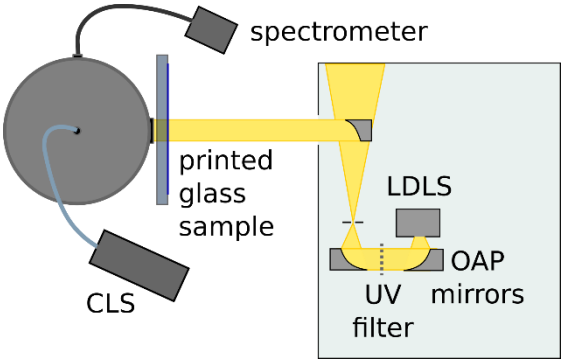

Figure 3: Setup for transmittance measurements

2.4. Measurements of transmittance

Transmittance measurements again use the same light source described in Section 2.2, adding a 6” integrating sphere directly into the collimated light path. Here, the full diameter of collimated light, 1.5”, is used. As shown in Figure 3, a correction light source (CLS), an OceanOptics DH2000 halogen-deuterium lamp, is connected using a 400-µm optical fiber to the secondary port of the integrating sphere to allow compensation for back-reflections from the sample. Spectra of the transmitted light are acquired using the aforementioned OceanOptics QE65000 spectrometer, connected via a 600-µm optical fiber to the baffled port of the integrating sphere.

Measurements are carried out for all samples with an integration time of 2.5 seconds and averaging over 5 measurements. In addition to measurements with the LDLS and dark background acquisitions, measurements with the CLS are carried out. Additionally, spectra without any samples mounted are acquired for reference purposes.

The transmittance through measured samples is calculated according to the following equation to compensate for back-reflections from the glass surface to the inside of the integrating sphere [6]. Here ϕ_x refers to measurements with the coated sample in place, while ϕ_0 refers to reference measurements without any samples:

$$T_x = \frac{\phi_{LDLS,x}}{\phi_{CLS,x}} \frac{\phi_{CLS,0}}{\phi_{LDLS,0}}$$

2.5 Refractive index and extinction coefficient estimation

Using the spectral reflectance, the refractive index can be estimated according to the following Fresnel equation for normal incidence, giving the following relationship for a single interface between medium 0 and medium x:

$$R_{0\to x} = \left| \frac{n_{\lambda,0} - n_{\lambda,x}}{n_{\lambda,0} + n_{\lambda,x}} \right|^2$$

While the inkjet-printed glass samples feature several interfaces, for an initial estimate of the refractive index of the ceramic ink, only the initial air-ink interface is considered.

In addition to the interface itself, absorption in the ink layer has to be considered. This absorption can be described by the extinction coefficient k derived from the Beer-Lambert Law. It can be estimated based on transmittance measurements and knowledge of the layer thickness:

$$T_\lambda = e^{-k_\lambda \frac{4\pi d}{\lambda}}$$

In this case, absorption in the glass substrate is neglected and the extinction coefficient is calculated based on the full transmittance of the printed samples.

2.6 Ray-tracing simulations and processing

The optical stack in the colored samples is simulated in OpticStudio by Zemax with the following simplifications: All surfaces are considered to be flat and all objects to have a constant thickness. Additionally, reflections on the detector surface, representing the PV cell or backsheet, are neglected. The model is outfitted with detectors for transmitted light (located within the encapsulant) and reflected light.

Ray-tracing simulations are carried out for incidence angles from 0° to 80° in 1° steps and for wavelengths ranging from 320 to 1100 nm in 10 nm steps. For each configuration, 1000 rays of randomized polarization are generated and traced through the optical stack, splitting rays into reflected and transmitted components at each interface.

The flux incident on each of the detectors is obtained through analysis of the exported ray paths in MATLAB, averaged over wavelengths and compared for different angles, to give a total, angular dependent transmittance analogous to the IAM.

2.7 IAM impact simulations

In order to estimate the impact of IAM differences on the annual yield of BIPV installations, a simulation tool based on weather data is developed in MATLAB.

At a chosen location, the angle of incidence for direct and ground reflected light are calculated, as well as an effective incidence angle for diffuse light based on the installation tilt. [7] Direct and diffuse irradiance data for a typical meteorological year (TMY), obtained from PVGIS (ec.europa.eu/jrc/en/pvgis), are then multiplied by the IAM for each timestamp using a 5th-order polynomial fit to the calculated incidence angle.

The recomposed irradiance is then compared for modules with and without ceramic ink printing on the inside of the glass, resulting in a measure for the additional, color dependent annual reflection losses.

For exemplary purposes, calculations are carried out for Risø, Denmark (55.7°N, 12.1°E) and Syracuse, Italy (37.1°N, 15.2°E) and five different configurations with installation tilt ranging from horizontal to vertical.

3 RESULTS

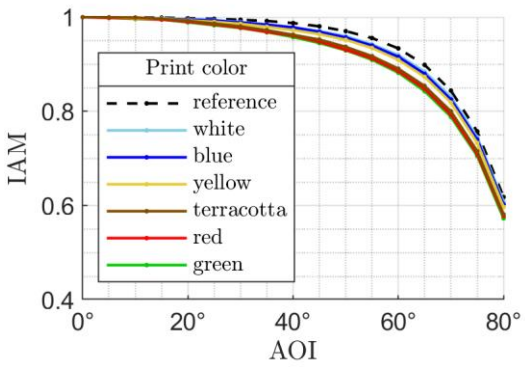

Figure 4: Measured absolute IAM

3.1 IAM Measurements

The results of the IAM measurements can be seen in Figure 4, showing the absolute IAM for incidence angles of 0° to 80°. Most noticeably, all colors show a significantly reduced IAM compared to the unprinted reference already at intermediary incidence angles, with highest losses for the red, green and terracotta colored samples. In contrast, the white, blue and yellow samples show a significantly lower reduction. This difference in colors becomes even more apparent in Figure 5, showing the relative IAM compared to the unprinted reference.

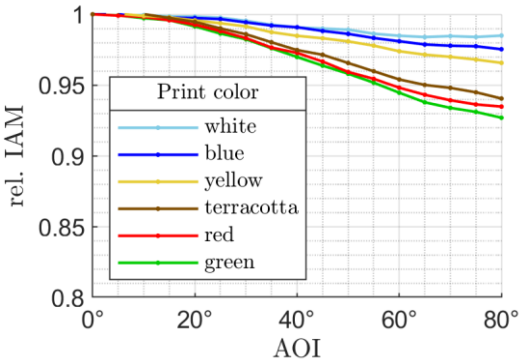

Figure 5: Measured relative IAM

Compared with measurements of the short-circuit current and/or maximum power of the PV cells as published previously [3], no direct correlation between relative IAM and total solar-weighted transmittance losses can be observed, as shown in Figure 6.

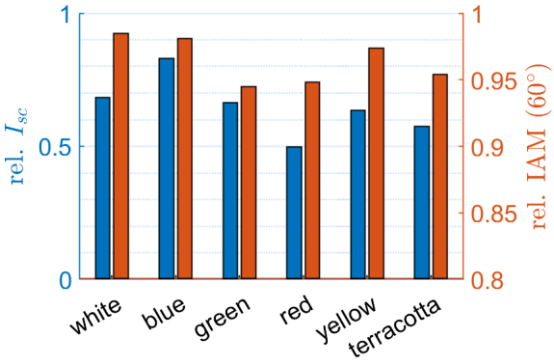

Figure 6: Comparison of relative Isc and relative IAM

3.2 Reflectance and transmittance

Both reflectance and transmittance are measured according to the descriptions in section 2.3 and 2.4. The resulting spectra are shown in Figures 7 and 8 respectively, showing the expected spectral variations for different colors.

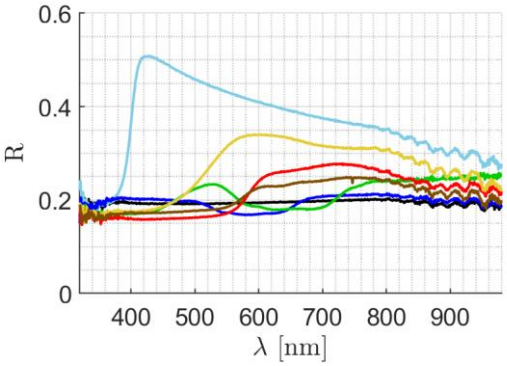

Figure 7: Measured spectral reflectance (see Figure 4 for legend)

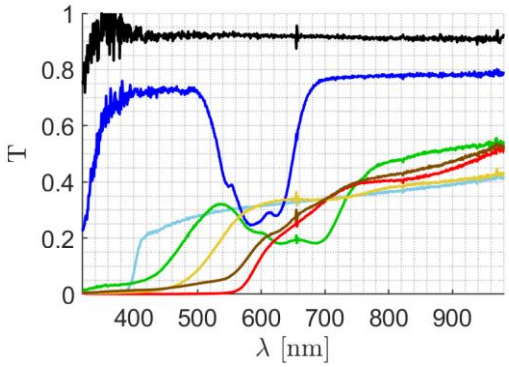

Figure 8: Measured spectral transmittance (see Figure 4 for legend)

Of special note is the blue colored sample, showing vastly increased transmittance compared to all other samples and low reflections over the entire spectrum. This can most likely be attributed to the specific pigment used in the ceramic ink, having different properties from those of the remaining colors.

3.3 Estimated refractive index

Figure 9 and 10 show the refractive index and extinction coefficient estimated from the reflectance and transmittance spectra. Beyond 980 nm, both n and k are extrapolated as constant values.

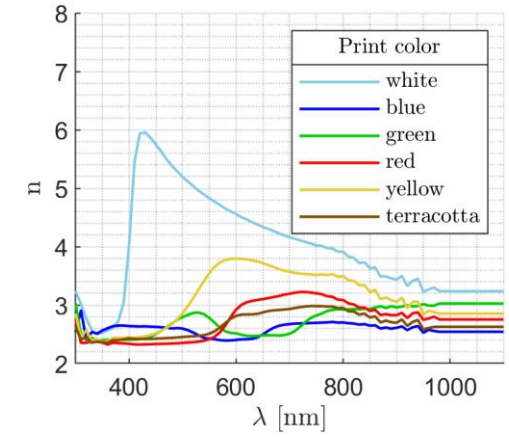

Figure 9: Estimated refractive index

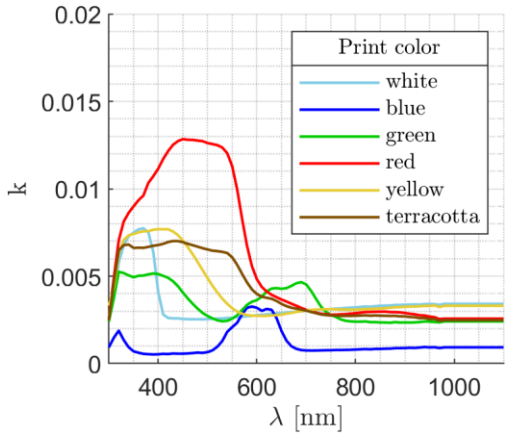

Figure 10: Estimated extinction coefficient

3.4 Raytracing results

The simulated absolute and relative IAM are shown in Figures 11 and 12 respectively. Immediately apparent are the oscillations in IAM over incidence angles, which can be attributed to variations in reflectance and transmittance at interfaces for differently polarized light as well as to interference effects between the wavelength of light and the thickness of the ink layer, differing only by approximately one magnitude. Accordingly, these effects are only visible in the raytracing simulations since no light scattering is considered, as diffuse light normally compensates for any spectral oscillations

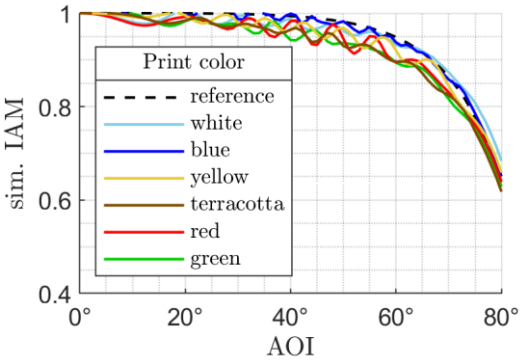

Figure 11: Simulated total IAM

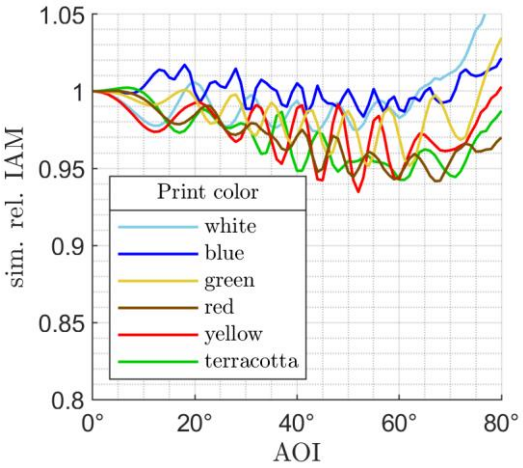

Figure 12: Simulated relative IAM

Apart from the oscillations, the simulated IAM curves generally agree well with the measurements, regarding both magnitude and trends for different colors. Only at high incidence angles does the simulation overestimate the IAM. This could possibly be attributed to changes in the reflectance and/or scattering behavior at high incidence angles, which are not considered in the simulation.

3.5 Yield simulations

For both locations, depending on color and installation tilt, the additional annual IAM losses range between approximately 1-5%, as can be seen in Figures 13 and 14.

For vertical installation, e.g. in façades, the worst performing colors show losses of more than 4%, and for the terracotta color, commonly used to mimic clay roof tiles, losses of up to 3% are evident for common roof tilts. Therefore, coloration dependent IAM losses can significantly affect BIPV system performance.

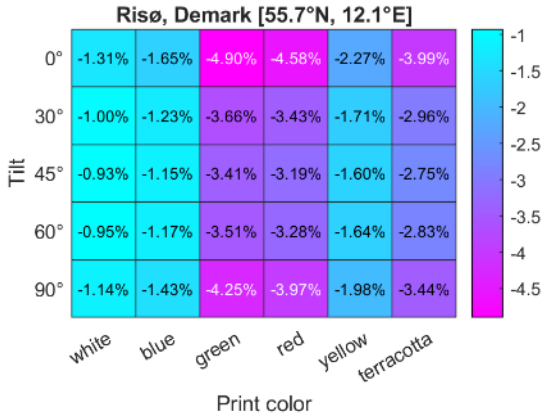

Figure 13: Annual additional reflection losses due to coloration in Risø, Denmark

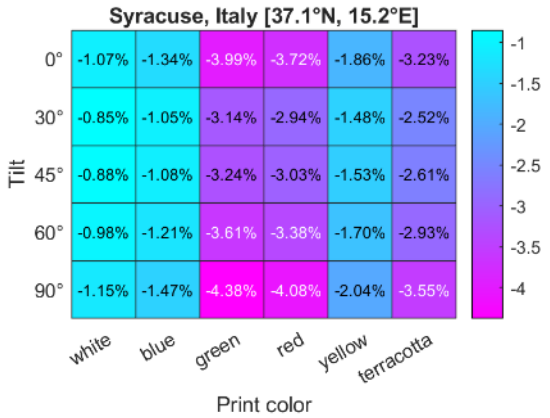

Figure 14: Annual additional reflection losses due to coloration in Syracuse, Italy

4 DISCUSSION

4.1 Other factors influencing the optical transmission

Changes in the IAM due to color could also be attributed to differences in light scattering, both for transmitted and reflected light. The diffusing properties of the ceramic inks may very well differ between colors, leading to different amounts of diffuse and specular components. Measurements of the bi-directional reflectance distribution function (BRDF) indicate a possible correlation between reflectance or transmittance specularity with the IAM. [3]

In addition, fluorescence effects may explain the very high reflectance of the white ink in Figure 6. Since a broadband light source is used for all spectral measurements, fluorescence cannot be identified from the measurements and may lead to errors in the estimated refractive index.

Finally, interactions between the pigments in the ceramic ink and the glass surface may affect the accuracy of results. During the thermal fusing of glass and ink, pigments may diffuse into the glass substrate, creating a refractive index gradient throughout the interface. Furthermore, pigment particle sizes may have an influence through interactions with light, leading to increased absorption or scattering.

4.2 Power yield estimations and PV module testing

As shown in section 3.5, the choice of color can have a significant impact on the annual yield of BIPV installations due to the differences in IAM. This has implications for both estimations and simulations of the power yield as well as for manufacturing and testing of BIPV products:

First of all, the choice of coloration has to be taken into account when estimating BIPV system performance. While the impact of coloration materials on the overall transmittance is well established, these observations indicate a requirement of new IAM measurements for every new color selection.

Secondly, these IAM measurements have to be made accessible for yield simulations, as otherwise BIPV system performance may be significantly overestimated. Furthermore, software used for BIPV yield prediction must accommodate more accurate modelling of the IAM to allow for accurate results.

5 CONCLUSIONS

In this work, the refractive index of ceramic inks used in colored BIPV modules was estimated and used in raytracing simulations to model the IAM. The simulations showed a high correlation between refractive index and IAM, indicating that the refractive index is one of the major driving force for these differences.

As alternative factor leading to different IAM, the diffusing properties of the ceramic inks, leading to light scattering, may be considered. As a next step, light scattering will be implemented in the raytracing model based on BRDF measurements to include these properties as well.

Finally, annual yield simulations have been shown that indicate additional reflection losses in colored BIPV modules of up to 5%, depending on color choice, location and orientation, compared to uncolored modules.

6 ACKNOWLEDGEMENTS

The authors would like to acknowledge the support from EUDP as a funding agency for project “64019-0029 PV-ROCK-ROOF”. This work was made possible through the Zemax smart research program with the use of OpticStudio under the license number L112498.

7 REFERENCES

[1] BIPVboost, BIPV Solutions in Europe: Competitiveness Status & Roadmap towards 2030 – White Paper, Report, Becquerel Institute (2021)

[2] M.J. Guillén et al., Solar Skins: An opportunity for greener cities, Report, SolarPower Europe and ETIP PV (2019)

[3] M. Babin, A.A. Santamaria Lancia, S. Thorsteinsson, A. Thorseth, Characterisation of Angular Dependent Optical Properties of Different Coloring Technologies Employed in BIPV Products, 37th EUPVSEC (2020) pp. 1136-1142

[4] Photovoltaic (PV) module performance testing and energy rating – Part 2: Spectral responsivity, incidence angle and module operating temperature measurements, Standard, IEC 61853-2:2016 (2016)

[5] N. Riedel Lyngskær et al., Interlaboratory Comparison of Methodologies for Measuring the Angle of Incidence Dependence of Solar Cells, 35th EUPVSEC (2018) pp. 1034-1039

[6] A. Tirpak, R. Young, Accurate transmission measurements of translucent materials, Report, Optronic Laboratories (2008)
[7] M.J. Brandemuehl , W.A. Beckman, Transmission of diffuse radiation through CPC and flat plate collector glazings, Solar Energy vol. 24, no. 5 (1980) pp. 511-513